CISM COURSES AND LECTURES NO. 489
INTERNATIONAL CENTRE FOR MECHANICAL SCIENCES

WAVES IN GEOPHYSICAL FLUIDS

TSUNAMIS, ROGUE WAVES, INTERNAL WAVES AND INTERNAL TIDES

EDITED BY

JOHN GRUE
KARSTEN TRULSEN

SpringerWienNewYork

SpringerWienNewYork

CISM COURSES AND LECTURES

The series presents lecture notes, monographs, edited works and proceedings in the field of Mechanics, Engineering, Computer Science and Applied Mathematics.
Purpose of the series is to make known in the international scientific and technical community results obtained in some of the activities organized by CISM, the International Centre for Mechanical Sciences.

INTERNATIONAL CENTRE FOR MECHANICAL SCIENCES

COURSES AND LECTURES - No. 489

WAVES IN GEOPHYSICAL FLUIDS

TSUNAMIS, ROGUE WAVES, INTERNAL WAVES AND INTERNAL TIDES

EDITED BY

JOHN GRUE AND KARSTEN TRULSEN
UNIVERSITY OF OSLO, NORWAY

SpringerWienNewYork

This volume contains 172 illustrations

Printed in Italy
SPIN 10817628

All contributions have been typeset by the authors.

ISBN-10 3-211-37460-4 SpringerWienNewYork
ISBN-13 978-3-211-37460-3 SpringerWienNewYork

Preface

This volume – *Waves in Geophysical Fluids* – contains extended versions of the lectures that were given at a summerschool in Centre International des Sciences Mécaniques (CISM), Udine, Italy, during the week of 11-15 July 2005. The subjects of the school covered: the formation of the very long *tsunamis*, the much shorter *rogue waves* taking place on the sea surface, very large *oceanic internal waves* and, finally, *internal tides and hot spots* in the ocean. The subjects were chosen because of their implications to the safety of human activity in and in relation to the ocean environment, and the impact of the processes to the ocean currents and climate. The physical phenomena and how to mathematically and numerically model them were described in the lectures.

The giant and destructive tsunami that occurred in the Indian Ocean on the 26th December 2004 urged scientists to communicate to the authorities and public the existing knowledge of tsunami wave modelling, and how the forecasts can be used for warning and evacuation of the people in the near shore region, corresponding to what is practice along the coasts of the Pacific Ocean. The first chapter of this book is precicsely describing the current practice of the forecasting and risk evaluation of tsunamis, and includes also an overview of the geograpical distribution of tsunami sources in the world's oceans. The mathematics and numerics behind the computations are described, including formulas for the tectonic generation, land slides and explosions, the typical length scales and magnitude of the resulting waves, and run-up on the coastline.

A prominent ship-owner said, during a visit to the hydrodynamic laboratory at the University of Oslo: "I have lost many men". He was speaking about how the *extreme – or rogue – waves* at sea had caused the loss of several of his ships. The extreme waves, like the Camille and Draupner waves, typically about 200 m long, are capable of lifting the sea surface almost 20 m above the level of equilibrium and causing a forward velocity of the water particles of more than 14 m/s, or 50 km/hour. The waves are caused by various physical mechanisms, which share a common factor, namely, focussing. A stochastic description based on Monte–Carlo simulations using deterministic models is given in chapter two. A deterministic description of focussing mechanisms is given in chapter three. The description is supplemented by a variety of nonlinear wave models, including analytical breather formulas. A novel fully nonlinear wave model in three dimensions is useful for rapid and accurate calculations of rogue waves, and compares favourably with PIV experiments (chapter four). The velocities and Lagrangian accelerations of the Draupner wave are estimated. The chapter culminates with numerical predictions of various crescent wave patterns in steep waves, and the competition between class I and class II instabilities.

Very large oceanic internal waves are a common phenomenon in all of the world's oceans. The full story about these waves is given in chapter five, including the discovery of the waves four decades ago, how the waves are visible from above through the signatures on the sea surface, and how to compute them. The strong interaction between the deep thermoclines in the ocean and the shelf slope causes strong near-bed currents. This is a factor that needs to be accounted for when it comes to new offshore installations in deep water, like the Ormen Lange gas field of Norsk Hydro at the slope of the Norwegian continental shelf. Weakly and fully nonlinear models of the waves are described including visualizations.

Energetic internal tides – hot spots – are formed by the barotropic tide interacting with submarine ridges and shelves, such as, *e.g.*, the Mid-Atlantic Ridge. Observations from several field campaigns in all parts of the world's oceans, and interpretation of the data including the description of spectra, are given in chapter six. The observation and the modeling of extreme internal tide generation at near critical latitudes in the Barents Sea as well as in, *e.g.*, the Strait of Gibraltar are described. The consequences of the internal tidal motion on the ocean currents and the climate, through the internal breaking and production of turbulent motion in the ocean, are elaborated.

We are grateful to Professor Manuel Velarde of Universidad Complutense de Madrid for suggesting us to submit a proposal for this summer school, and to the Rectors of CISM for approving it, giving us also the chance to prepare the material for this book. The school could not have been realized without the rather generous support from CISM and also by the economical support from the Strategic University Program: Modelling Waves and Currents for Sea Structures 2002-6 at the University of Oslo, funded by the Research Council of Norway.

Oslo and Marseille, May 2006

John Grue and Karsten Trulsen

CONTENTS

3

Freak waves phenomenon: Physical mechanisms and modelling

5

Very large internal waves in the ocean – observations and nonlinear models
by John Grue 205

6

Hydrodynamics of Tsunami Waves

Efim Pelinovsky
Laboratory of Hydrophysics,
Institute of Applied Physics
Nizhny Novgorod, Russia

Abstract The giant tsunami that occurred in the Indian Ocean on 26th December 2004 draws attention to this natural phenomenon. The given course of lectures deals with the physics of the tsunami wave propagation from the source to the coast. Briefly, the geographical distribution of the tsunamis is described and physical mechanisms of their origin are discussed. Simplified robust formulas for the source parameters (dimension and height) are given for tsunamis of different origin. It is shown that the shallow-water theory is an adequate model to describe the tsunamis of the seismic origin; meanwhile for the tsunamis of the landslide or explosion origin (volcanoes, asteroid impact) various theories (from linear dispersive to nonlinear shallow-water equations) can be applied. The applicability of the existing theories to describe the tsunami wave propagation, refraction, transformation and climbing on the coast is demonstrated. Nonlinear-dispersive effects including the role of the solitons are discussed. The practical usage of the tsunami modeling for the tsunami forecasting and tsunami risk evaluation is described. The results of the numerical simulations of the two global tsunamis in the Indian Ocean induced by the catastrophic Krakatau eruption in 1883 and the strongest North Sumatra earthquake in 2004 are given.

1 Introduction

After the catastrophic tsunami in the Indian Ocean occurred on December 26, 2004 everybody knows the Japanese word "tsunami" meaning "harbor wave". Now tsunami waves are defined as surface gravity waves that occur in the ocean as the result of large-scale short-term perturbations: underwater earthquakes, eruption of underwater volcanoes, submarine landslides, underwater explosions, rock and asteroid falls, avalanche flows in the water from "land" mountains and volcanoes, and sometimes drastic changes of weather conditions (Murty, 1977; Pelinovsky, 1982, 1996; Bryant, 2001). The characteristic parameters of tsunamis are: duration, 5 to 150 min, length, 100 m to 1000 km, speed propagation, 1 to 200 m/s, and their heights can be up to tens of meters. Various data of observations in the world's oceans can be found in catalogues (Soloviev et al., 1988, 2000; Lander and Lockridge, 1989; O'Loughlin and Lander, 2003), and in sites of the National Geophysical Data Center - NGDC (http://www.ngdc.noaa.gov) and the Tsunami Laboratory (http://tsun.sscc.ru/htdbpac/). Most of them (more than 1000) occurred in the Pacific, and about 100 - in the Atlantic and Indian Oceans. Earthquakes

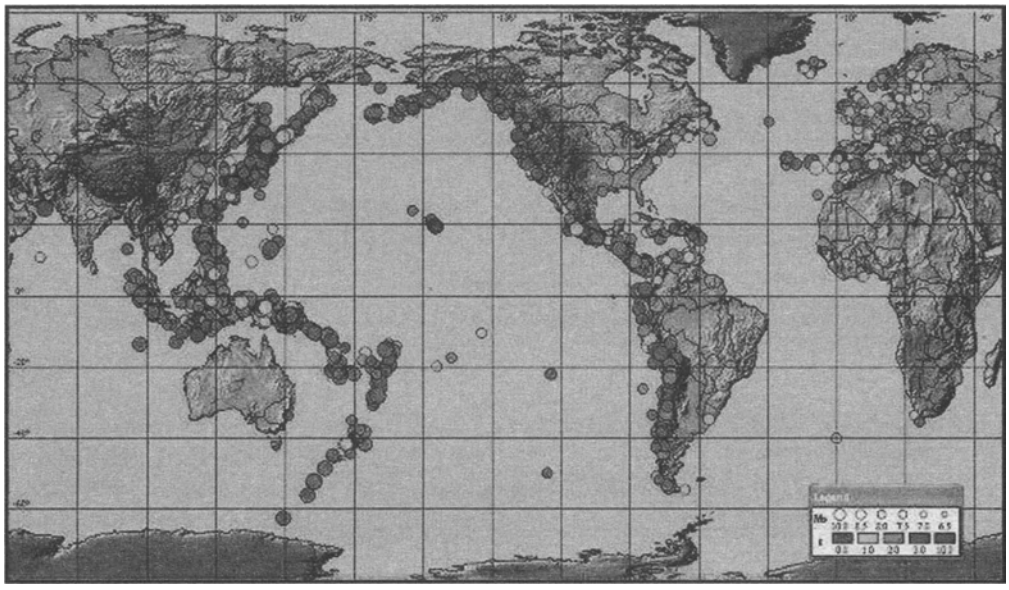

Figure 1. Geographical distribution of tsunami sources in the world's oceans. The size of circles is proportional to the earthquake magnitude, density of gray tone - to the tsunami intensity.

are responsible for 75% of all events, and their geographical distribution is shown in figure 1 (Gusiakov, 2005). A great attention is paid to tsunamis, which can occur due to the possible asteroid impact (diameter 100 m - 50 km) in the ocean, and the number of documented events exceeds 10 (figure 2).

By the number of deaths tsunami waves are in the fifth place after earthquakes, floods, typhoons and volcanic eruptions (very rough estimates). However, tsunamis have a high destructive potential for countries on large distances from the source, as it was demonstrated on December 26, 2004 when tsunami waves killed more than 250,000 people in Indonesia, Thailand, Sri Lanka, India, the Maldives, Kenya and Somali. Approximately 10 events occurred each year, and 10% of them are really damaging tsunamis (figure 3).

Short- and long-term tsunami predictions require complex studies of the mechanisms of tsunami excitation, the adequate modelling of tsunami propagation and the climbing on a beach, and the subsequent development of tsunami risk maps. This lecture deals with the hydrodynamics of the tsunami waves for all stages of tsunami propagation from the source to the coast.

2 Parameters of tsunami waves in the source

The determination of the tsunami wave characteristics in the source is an extremely difficult problem of the geophysics. Taking into account that the main goal of our study is

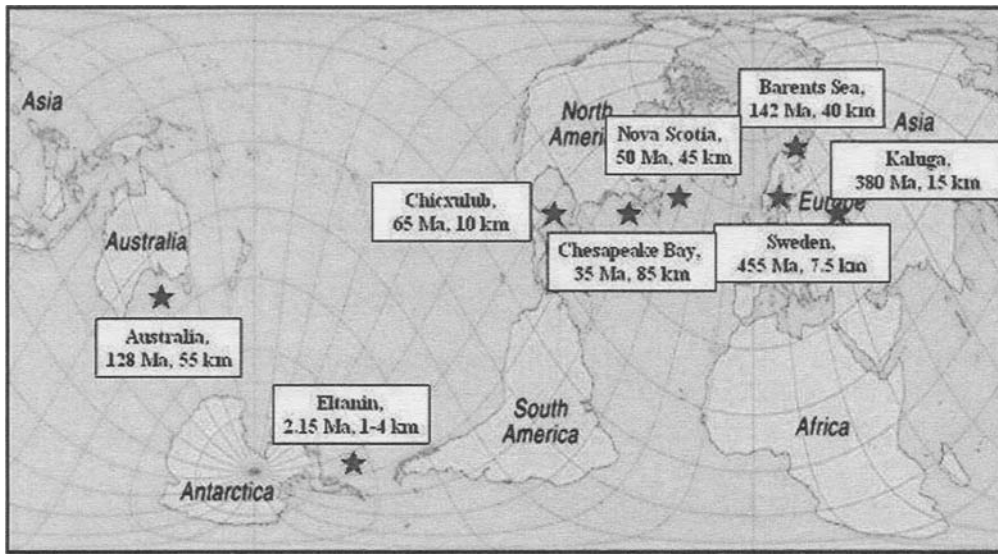

Figure 2. Map of known asteroid entries into the sea (Kharif and Pelinovsky, 2005).

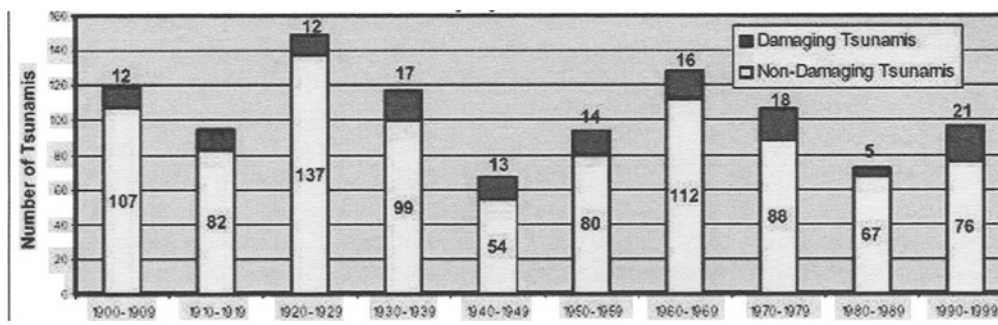

Figure 3. Tsunami statistics for the 20th century (NGDC).

the hydrodynamic theory, we briefly reproduce here some rough formulas to demonstrate the order of magnitudes of the height and dimensions of the initial water displacement in the tsunami source.

2.1 Tsunamis of seismic origin

The parameters of the source of tsunami waves of the seismic origin depend on many earthquake parameters: the fault length and width, the orientation in space and focal depth. These can be determined from the seismic models by Manshinha and Smylie (1971) or Okado (1985). Approximately, the tsunami source has an elliptical shape. Its effective radius, R_e and water displacement, H_e can very roughly be estimated through the earthquake magnitude, M which characterizes the earthquake energy (Hatori, 1966;

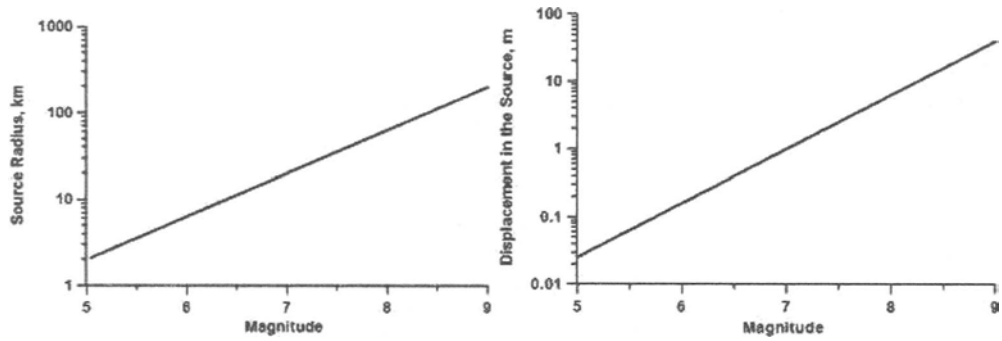

Figure 4. Rough estimates of the tsunami parameters in the source versus the earthquake magnitude.

Mirchina et al., 1982)

$$\log R_e = 0.5M - 2.2, \qquad \log H_e = 0.8M - 5.6 \tag{2.1}$$

where R_e is in km, H_e in m and M is measured in the Richter scale. They are displayed in figure 4. It is clearly seen, that the strong earthquakes with magnitudes 7-9 generate big tsunami waves several meters in height and one hundred km in length. For instance, the source of the last giant 2004 tsunami in the Indian Ocean (magnitude 9.0-9.3) had the following approximate dimensions: length, 1300 km; width, 200 km; and height, 15 m - these values correspond to the estimates in (2.1). Of course, the accuracy of these estimates is very low and here they are given to demonstrate the characteristic scales of the tsunami source only. They show that tsunamis of seismic origin are shallow-water waves, and that the dispersion parameter, $\mu = h/\lambda$ is small. Here h is the basin depth and λ the characteristic wavelength. The shape of tsunami waves in the source were in the early papers considered as a displacement of one polarity (like an ellipsoid). Nowadays components of opposite polarities appear in the shapes, in accordance with seismic solutions (Manshinha and Smylie, 1971; Okado, 1985); see also Synolakis et al. (1997).

2.2 Tsunamis from underwater explosions

Since the description of the mechanism of wave formation during an explosion, as such, is an extremely complicated problem, the main attention here is given to the choice of the equivalent source that gives the possibility to explain the wave field on long distances. The definition parameter for the deep-water explosion is the energy, and this characteristic can be used for tsunami waves generated by the explosion eruption of underwater volcanoes. Detailed experiments have been performed with underwater explosions with low energies (10^6 Joules), when the generated waves have small wavelengths compared with the water depth (deep-water waves). The best agreement of the experimental data from weak explosions with the results of the linear dispersive theory is achieved, when

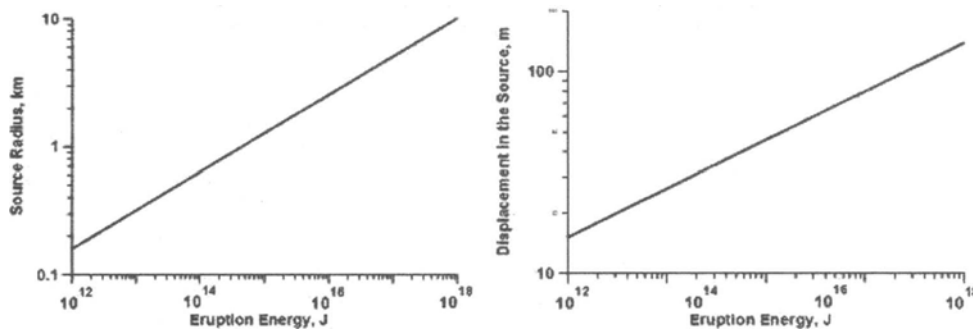

Figure 5. Parameters of the tsunami source of explosion origin.

the equivalent source has a shape of parabolic cavity with dimensions (Le Mehaute and Wang, 1996)

$$R_e = 0.04E^{0.3}, \qquad H_e = 0.02E^{0.24}, \tag{2.2}$$

where E is the explosion energy in Joules and R_e, H_e are in meters. These formulas are presented in figure 5. Formally, they should be used for deep water only but may also be applied for water of finite depth. For instance, the 1952-1953 Mijojin underwater volcano eruptions had an energy of 10^{16} J, and the parameters of the tsunami source were, $R_e \sim$ 2-3 km, $H_e \sim$ 100-200 m. In fact, due to cylindrical divergence the wave amplitude attenuates very quickly, and it is less than 10 m at distances of 30 km. For the 1883 Krakatau eruption ($8.4 \cdot 10^{17}$ Joules) the initial dimensions of volcano caldera are estimated as $R_e \sim 3.5$ km, and $H_e \sim 220$ m (Bryant, 2001). Such dimensions of the Krakatau tsunami source are chosen knowing the characteristics of volcano eruption without no using of (2.2). Thus, the tsunami waves from underwater volcano should be considered in general as the waves in the basin of finite depth.

The similar estimates are used for tsunami source of asteroid origin (Ward and Asphaug, 2000). Asteroids larger than 200 meters in diameter hit the Earth about every 3000-5000 years, so the probability of one impacting in a given human lifetime is about 2-3% (Hills and Gods, 1998). The cavity radius and depth depends from on the impactor radius and the "entry" velocity, and for typical conditions they are presented in figure 6 (Ward and Asphaug, 2000). Such waves also should also be considered as the waves in water of finite depth.

All classes of existing water theories may be used to explain the tsunami waves from underwater explosions: linear dispersive theory (Ward and Asphaug, 2000, 2003), shallow water simulations (Mader, 1998; Choi et al., 2003), and fully nonlinear computations (Crawford and Mader, 1998). For waves in an intermediate-depth basin, the shallow-water results overestimate the tsunami parameters to compare with simulations in the framework of incompressible Navier-Stokes equations (Crawford and Mader, 1998).

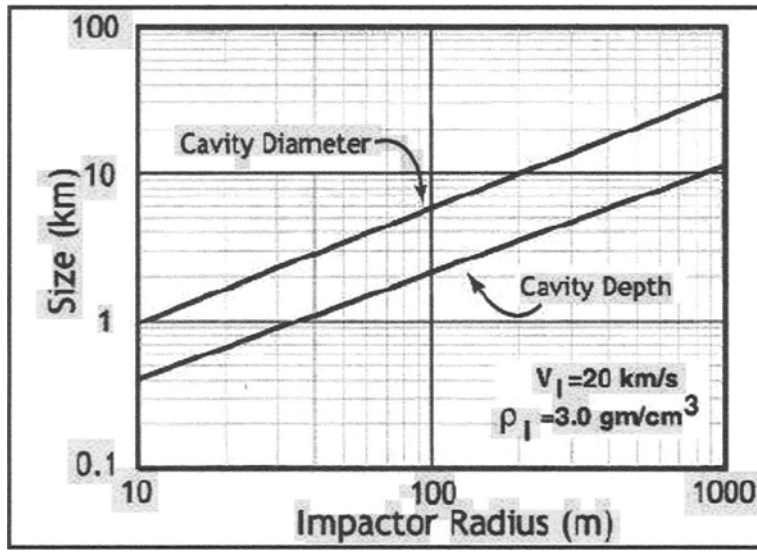

Figure 6. Characteristics of the equivalent source of asteroid tsunami.

2.3 Tsunamis generated by landslides

Parameters of submarine landslides as well as rock falls and the debris avalanches from "land" volcanoes vary within wide limits; they induce tsunami waves of different scales (Watts, 2000). As a result, all classes of theoretical models are applied here, they are, linear dispersive equations (Ward, 2001), nonlinear-dispersive Boussinesq system (Watts et al., 2003), nonlinear shallow-water equations (Assier-Rzadkiewicz et al., 2000) and fully nonlinear and dispersive computations (Grilli et al., 2002).

The data given above show the various scales of tsunami waves in the ocean. Earthquakes typically induce the large-scale waves (up to 1000 km) and the basic model for them is the shallow-water system. Tsunamis of the relatively weak explosion origin (underwater volcano eruptions, asteroid impact) are typically short-scales waves (0.1-1 km) and here the linear dispersive theory is the basic model. Many earthquakes initialize a submarine landslide motion, which then generates intense tsunami waves. This problem was the subject of the special discussion on the NATO Workshop (Yalciner et al., 2003). Tsunamis from landslides depending of characteristic scales can be described by one of these models. Due to strong variability of the ocean seafloor, the ratios depth/wavelength and amplitude/depth are changed along the wave path, and different theoretical models can be applied for the different stages of the wave propagation: in the source, in the open sea, in the coastal zone and on the beach. Typical models of tsunami waves will be discussed in the next sections.

3 Shallow water equations

The governing hydrodynamic model of tsunami generation by the underwater earthquake is based on the well-known Euler equations of ideal incompressible fluid

$$\frac{\partial \mathbf{u}}{\partial t} + \mathbf{u} \cdot \nabla_1 \mathbf{u} + w\frac{\partial \mathbf{u}}{\partial z} + \frac{\nabla_1 p}{\rho} = 0, \tag{3.1}$$

$$\frac{\partial w}{\partial t} + \mathbf{u} \cdot \nabla_1 w + w\frac{\partial w}{\partial z} + \frac{1}{\rho}\frac{\partial p}{\partial z} = -g, \tag{3.2}$$

$$\nabla_1 \cdot \mathbf{u} + \frac{\partial w}{\partial z} = 0. \tag{3.3}$$

with corresponding boundary conditions at the bottom and ocean surfaces (the geometry of the problem is shown in figure 7):

at the sea bottom ($z = -h(x, y, t)$),

$$w - \mathbf{u} \cdot \nabla_1 h = W_n(x, y, t), \tag{3.4}$$

at the free surface ($z = \eta(x, y, t)$), the kinematic condition is

$$w = \frac{\mathrm{d}\eta}{\mathrm{d}t} = \frac{\partial \eta}{\partial t} + \mathbf{u} \cdot \nabla_1 \eta, \tag{3.5}$$

and the dynamic equation,

$$p = p_{atm}. \tag{3.6}$$

Here $\eta(x, y, t)$ is the water displacement, $\mathbf{u} = (u, v)$ and w are horizontal and vertical components of the velocity field, x and y are coordinates in the horizontal plane, z-axis is directed upwards vertically, ρ is water density, p is pressure and p_{atm} is the atmospheric pressure, which is assumed constant, g is gravity acceleration, $h(x, y, t)$ is variable ocean depth due to the bottom displacement in the source area, and W_n is the velocity of the bottom motion on the perpendicular direction (when the bottom motion is vertical only, W coincides with $\mathrm{d}h/\mathrm{d}t$). The differential operator ∇_1 acts in the horizontal plane.

These equations can be applied to study tsunamis generated by bottom displacements in the source of underwater earthquake or submarine landslides. In the last case the function $h(x, y, t)$ can be given only for a solid-body landslide. In the opposite case, the equations of the slide motion should account the rheology of the landslide material (Kulikov et al., 1996; Heinrich et al., 1998).

As pointed out above, the tsunami waves from strong underwater earthquakes are long (as compared to the ocean depth). Therefore, it is natural first to consider the long-wave (or shallow-water) approximation as a model of tsunami generation, and then estimate the conditions of its applicability. The theory of long waves is based on the main assumption that the vertical velocity and acceleration are low as compared to horizontal ones and can be calculated from the initial system with the help of an asymptotic procedure. As small parameter it uses the ratio between the vertical velocity and the horizontal one or the ocean depth to the characteristic wavelength and will be given below.

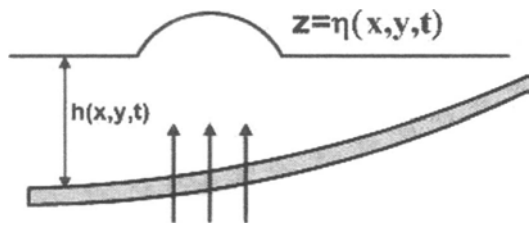

Figure 7. Problem geometry.

Here a simpler algorithm is used, which consists in neglecting vertical acceleration dw/dt in (3.2). In this case the equation (3.2) is integrated and, with the dynamic boundary condition (3.6) taken into account, determines the hydrostatic pressure:

$$p = p_{atm} + \rho g(\eta - z). \tag{3.7}$$

Substituting (3.7) into (3.1) and neglecting the vertical velocity once again, we obtain the first equation of the long-wave theory:

$$\frac{\partial \mathbf{u}}{\partial t} + \mathbf{u} \cdot \nabla_1 \mathbf{u} + g \nabla_1 \eta = 0. \tag{3.8}$$

The second equation is obtained by integration of (3.3) over the depth from the bottom ($z = h(x, y, t)$) to the surface ($z = \eta(x, y, t)$), taking into account boundary conditions (3.4) - (3.5), as well as the fact that the horizontal velocity does not depend on the vertical coordinate, z:

$$\frac{\partial \eta}{\partial t} + \nabla_1 \cdot [(h + \eta)\mathbf{u}] = W_n. \tag{3.9}$$

Equations (3.8) - (3.9) are closed as related to the functions η and $\mathbf{u}$. They are *nonlinear* (the so-called nonlinear shallow-water theory), *inhomogeneous* (the right-hand part is non-zero), and contain a preset function h that is variable in time and space.

Most generally used within the tsunami problem is the linear version of the shallow-water theory. In this case variations of depth are assumed weak, as well as the velocity of the bottom motion. As a result, we obtain a linear set of equations:

$$\frac{\partial \mathbf{u}}{\partial t} + g \nabla_1 \eta = 0, \qquad \frac{\partial \eta}{\partial t} + \nabla_1 \cdot (h\mathbf{u}) = W_n \tag{3.10}$$

with the right-hand part $W_n(x, y, t)$. It is convenient to exclude the velocity and pass over to the wave equation for the surface elevation:

$$\frac{\partial^2 \eta}{\partial t^2} - \nabla_1 \cdot (c^2 \nabla_1 \eta) = \frac{\partial W_n}{\partial t}, \tag{3.11}$$

where

$$c(x,y,t) = \sqrt{gh(x,y,t)} \tag{3.12}$$

is the long-wave speed (upper limit for the surface waves). The equation (3.11) is the basic one within the linear theory of tsunami generation and must be supplemented by initial conditions. It is natural to believe that at the initial moment the ocean is quiet, i.e.

$$\eta = 0, \quad \mathbf{u} = 0 \quad \text{or} \quad \partial\eta/\partial t = 0, \tag{3.13}$$

though due to linearity of (3.11) a more general case of the initial conditions can be also considered. From the point of view of mathematical physics the wave equation (3.11) is too well studied to discuss the details of its solution here. Note only that since the function W_n is "switched on"' at the moment $t = 0$, we formulate here the Cauchy problem for the wave equation in a generalized sense, i.e., we include into the consideration the generalized functions and do not require that the level and flow velocity should be differentiated twice.

The initial and long-wave systems of the equation presented here are basic hydrodynamic models of tsunami generation by underwater strong earthquakes and giant landslides.

4 Tsunami generation and propagation in the shallow sea of constant depth (linear approximation)

The simplest model here uses the linear wave equation (3.11) with the preset right-hand part $W_n(x,y,t)$. We can identify W_n with the vertical velocity of the bottom motion (dz_b/dt). In this case (3.11) is reduced to the classical wave equation

$$\frac{\partial^2\eta}{\partial t^2} - c^2\triangle\eta = \frac{\partial^2 z_b}{\partial t^2} \tag{4.1}$$

with constant long-wave speed, c and zeroth initial conditions.

Vertical bottom displacement. We will consider first a simple model of pulse perturbation when the bottom shifts momentarily to a finite value (the earthquake acts like a piston in this case)

$$h(x,y,t) = h_0[1 - \eta_0(x,y)\theta(t)], \tag{4.2}$$

where $\eta_0(x,y)$ describes the shape of the residual displacement of sea floor in the source and $\theta(t)$ is the Heaviside (unit) function with $\theta(t) = 1(t > 0)$ and $\theta(t) = 0(t < 0)$. Taking into consideration that $W_n = dh/dt$, the velocity of the bottom shift is the generalized Dirac function, $W_n = \eta_0\delta(t)$. It is easily shown in this case that the generalized Cauchy problem for the inhomogeneous wave equation is equivalent to the "usual" Cauchy problem for the homogeneous wave equation,

$$\frac{\partial^2\eta}{\partial t^2} - c^2\triangle\eta = 0 \tag{4.3}$$

with the following initial conditions

$$\eta(x,y,t=0)=\eta_0(x,y), \quad \frac{\partial\eta}{\partial t}(x,y,t=0)=0. \tag{4.4}$$

We observe, when the piston shift is instantaneous, the ocean surface rises to the value of the bottom shift. This is evident due to the incompressibility of the fluid and the pressure being hydrostatic. This is the simplest and most comprehensive model of wave excitation (from the physical point of view), and has found the wide usage in the study of tsunamis. The shape of initial bottom displacement is determined from the solution of the seismic problem, see for instance, Manshinha and Smylie (1971) and Okada (1985). Roughly, the parameters of the tsunami source of the seismic origin are given in section 2 through the earthquake magnitude.

The radiation pattern depends on the source shape (the influence of the bottom relief will be analyzed later). If the tsunami source is an ellipse with large eccentricity like an 1D strip, the wave field is obtained simply by

$$\eta(x,t)=\frac{1}{2}[\eta_0(x-ct)+\eta_0(x+ct)], \tag{4.5}$$

and the shape of the tsunami wave repeats the shape of the initial displacement, with the height reduced by a factor of two. For a two-dimensional source, the solution of (4.3) is described by the Poisson formula

$$\eta(\mathbf{r},t)=\frac{1}{2\pi c}\frac{\partial}{\partial t}\int\frac{\eta_0(\boldsymbol{\rho})\mathrm{d}\boldsymbol{\rho}}{\sqrt{c^2t^2-|\mathbf{r}-\boldsymbol{\rho}|^2}}, \tag{4.6}$$

where $\mathbf{r}$ and $\boldsymbol{\rho}$ are two-dimensional vectors in the (x,y) plane, and integration is performed over the region of the circle

$$|\mathbf{r}-\boldsymbol{\rho}|^2<c^2t^2. \tag{4.7}$$

This integral is not calculated in the general case. One analytical example of the circular wave is displayed in figure 8. The simplest asymptotic is found for the wave field at the source for long times ($t >> r/c$)

$$\eta(r,t)\sim-\frac{V}{2\pi c^2t^2}, \tag{4.8}$$

where V is the volume of the water displaced at the source

$$V=\int\eta_0(\mathbf{r})\mathrm{d}\mathbf{r}. \tag{4.9}$$

Thus, unlike in the one-dimensional case, when the wave leaves the source completely, a motion remains in the source the water displacement that is damped with time. It is important to mention that if the water only uplifts in the source, the wave contains a leading elevation accompanied by a depression. The depth of the depression depends on the steepness of the leading wave and may exceed its height. In the opposite case, if the

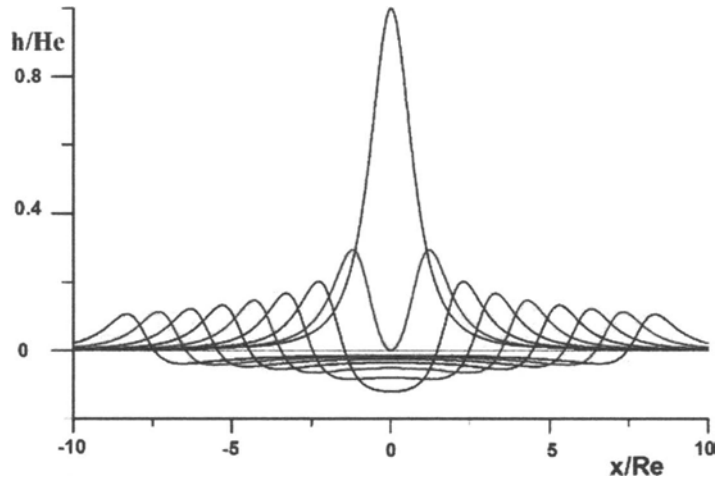

Figure 8. Cross-section of the circular wave for various times with unit R_e/c.

water falls in the source, the leading wave is negative (depression), but the next wave is positive with a higher amplitude. This explains why it is very dangerous to walk on the "open" seafloor when the water is receded; the next wave climbs on the beach.

Another asymptotic can be obtained for the amplitude of the leading wave, in particular for the elliptic uniform displacement in the source:

$$H = \frac{H_e}{2}\left(\frac{R}{d}\right)^{1/2}, \tag{4.10}$$

where R is radius of curvature of the ellipse at the point close to the observation, and d is the distance from the observation point to the center of the circle with curvature R^{-1}, which is r for large distance. Hence, the wave amplitude is attenuated as $r^{-1/2}$, but its value depends on the orientation of the source in relation to the observation point. Radiation directivity can be characterized by the ratio of the amplitude of the wave radiated towards the major axis H_a and the amplitude of the wave radiated towards the minor axis H_b. The latter is determined by the following simple equation obtained from (4.10)

$$\frac{H_a}{H_b} = \left(\frac{b}{a}\right)^{3/2}. \tag{4.11}$$

Thus, an elliptical source forms a radiation that is inhomogeneous in space. The strongest radiation is directed towards the minor axis of the ellipse. This position of the source, relative to the observation point, is the most dangerous as far as the formation of strong tsunami waves is considered. The sources of historical tsunami waves were mainly extended along the nearest coast, and, consequently, caused waves with larger amplitudes under other equal conditions.

The last conclusion concerns the arrival time. If the initial tsunami source is finite (η_0 is given only in the ellipse), the wave arrives at a given point r after a time $(r-R)/c$, i.e. it propagates with the speed, c. This is a conclusion that does not depend on the geometry of the problem, but is obtained by the shallow-water system being hyperbolic. This is of great importance for the prediction of the arrival time of tsunamis after an earthquake. More details are provided in section 8.

Landslide motion. Let us consider as source the simplest two-dimensional (x, z) bottom displacement as the model of a landslide moving horizontally with constant speed V. Actually, in this case we have the 1D problem: the solution, which satisfies the zeroth initial conditions, is easily found explicitly from (4.1)

$$\eta(x,t) = \frac{V^2}{V^2-c^2} z_b(x-Vt) - \frac{V^2}{2c(V-c)} z_b(x-ct) + \frac{V^2}{2c(V+c)} z_b(x+ct). \qquad (4.12)$$

This solution is a superposition of three waves: one of them is bounded, and the two others are free. After some time they separate in space: the first wave remains attached to the source zone (moving with a landslide), while the two others leave. Let us discuss first the field in the source for sufficiently long times, when the waves become separated in space; it is described by the first term in (4.12). We see that in the case of a large speed ($V \to \infty$) the surface elevation responds to the bottom displacement ($\eta \approx z_b$), and when the motion is slow due to small vertical acceleration, the surface level is practically not perturbed ($\eta \approx V^2 z_b/c^2$). The free wave moving in the direction of the landslide is similarly amplified (but it is a trough, not a crest). The wave leaving the landslide zone in the opposite direction is limited with respect to the amplitude at any velocity (that is caused by great difference in motion velocities) and this wave is weak. Of a special interest is the case of synchronism between the landslide motion and the excited wave, when even a small bottom displacement causes the strong water motion; formally, bounded and free waves propagate together and the resulting wave is

$$\eta(x,t) = -\frac{ct}{2} \frac{\partial z_b(x-ct)}{\partial x}. \qquad (4.13)$$

Let us consider now a model of the horizontally "growing" landslide, when its right end moves to the finite distance X, in such a way that the velocity of the bottom motion, V differs from zero only in the region $(0-X)$, see, figure 9

$$W_n = H_b \delta(t - x/V), \quad 0 < x < X. \qquad (4.14)$$

The solution of (4.1) is easily found in the form of the Duhamel integral

$$\eta(x,t) = \frac{1}{2c} \int_0^t \mathrm{d}\tau \int_{x-c(t-\tau)}^{x+c(t-\tau)} \mathrm{d}y \frac{\partial W_n}{\partial \tau}(y,\tau). \qquad (4.15)$$

Out of the source region the wave is constituted of two rectangular pulses moving in opposite directions. The amplitude and duration of the pulse moving towards ($x > 0$) are

$$H = \frac{H_b}{2} \frac{V}{|V-c|}, \qquad T = \frac{X}{c} \frac{|V-c|}{V}, \qquad (4.16)$$

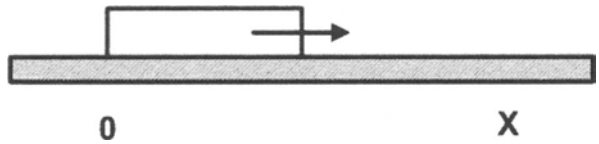

Figure 9. Moving landslide.

and in the opposite direction,

$$H = \frac{H_b}{2}\frac{V}{|V+c|}, \qquad T = \frac{X}{c}\frac{|V+c|}{V}. \tag{4.17}$$

It can be seen that here a resonance also takes place. When the speed of the bottom displacement motion, V approaches the velocity of wave propagation c, the amplitude of the resonance wave goes to infinity, and the pulse duration becomes very small. Such short pulses violate the applicability of the long-wave theory, and the resonance should be considered within more accurate models. Similar calculations can be made also for the plane (x, y) problem, when the bottom displacement runs within a rectangular region. It should be emphasized that the resonance is retained in the plane problem, wherein all the displacements with velocities higher than c are of a resonance character, and maximum radiation occurs along directions $\theta = \arccos(c/V)$, determined through the so-called Mach angle. Such relations are well-known in the theory of the wave radiation. Wave amplitude stays finite at $c \neq V$, and it is proportional to the factor $(1-c^2/V^2)^{-1/2}$ for the Mach direction.

Thus, horizontal motions of the bottom in the seismo-active zone or horizontally moving landslides cause intensification of the radiated waves. "Catastrophic" within the linear shallow-water theory is the case of resonance that occurs when $c = V$. The wave amplitude becomes then formally unbounded. This can explain how a weak earthquake sometimes generates a strong tsunami: at first the earthquake initiates a landslide motion which causes the water waves. The mechanism of the tsunami generation by submarine landslides is of great interest, and the special NATO workshop was recently organized (Yalciner et al., 2003).

5 Effects of finite depth for tsunami waves of seismic origin

Usually, the earthquake area has large dimensions (compared with water depth), and mainly shallow-water theory is used to describe the properties of tsunami waves. In principal., all results of the shallow-water theory can be re-examined using the finite-depth approximation for water waves. For instance, we may check the piston model of tsunami generation described in section 4. It is evident that the instantaneous bottom motion results in large values of the vertical velocity, in contrast to the assumptions of the shallow-water theory. Since the motion begins from the state of rest, the fluid motion can be considered to be potential. The equations for the fluid potential, $\Phi(x, y, z, t)$ can be easily derived from the Euler equations (3.1)-(3.6), and are well-known (for the fluid

of constant depth, linear approximation):
Laplace equation

$$\Delta\Phi + \frac{\partial^2\Phi}{\partial z^2} = 0, \qquad (-h < z < 0), \tag{5.1}$$

the boundary conditions on the sea surface ($z = 0$)

$$\frac{\partial^2\Phi}{\partial t^2} + g\frac{\partial\Phi}{\partial z} = 0, \tag{5.2}$$

and seafloor ($z = -h$)

$$\frac{\partial\Phi}{\partial z} = W_n(x, y, t). \tag{5.3}$$

The water displacement is expressed through potential as

$$\eta(x, y, t) = -\frac{1}{g}\frac{\partial\Phi}{\partial t} \quad \text{at} \quad z = 0. \tag{5.4}$$

The solution of this boundary problem can be found using the time-dependent Green function, G. The latter is a harmonic function in space with a peculiarity of the source type, and it is found analytically (Stoker, 1955)

$$G(\mathbf{r}, z, t|\mathbf{r}_0, z_0, \tau) = \frac{1}{h}\int_0^{+\infty} \frac{J_0(m|\mathbf{r} - \mathbf{r}_0|/h)}{\cosh(m)} \left\{\sinh\left[m\left(1 - \frac{z - z_0}{h}\right)\right] - \right.$$

$$- \sinh\left[m\left(1 + \frac{z + z_0}{h}\right)\right] + \frac{2m}{\gamma^2\cosh(m)}\left[1 - \right.$$

$$\left. \left. - \cos\left(\gamma\sqrt{g/h}(t - \tau)\right)\right]\cosh\left[m\left(1 + \frac{z}{h}\right)\right]\cosh\left[m\left(1 + \frac{z_0}{h}\right)\right]\right\} \mathrm{d}m, \tag{5.5}$$

where $\gamma = [m\tanh(m)]^{1/2}$. As a result, the water displacement induced by the bottom motion is determined by the integral

$$\eta(\mathbf{r}, t) = \frac{1}{4\pi g}\int\int \mathrm{d}\mathbf{r}_0 \int_0^t W_n(\mathbf{r}_0, t)\frac{\partial^2 G(\mathbf{r}, 0, t|\mathbf{r}_0, -h, \tau)}{\partial t\partial\tau}\mathrm{d}\tau, \tag{5.6}$$

where

$$G(\mathbf{r}, 0, t|\mathbf{r}_0, -h, \tau) = \frac{2}{h}\int_0^{+\infty} \frac{mJ_0(m|\mathbf{r} - \mathbf{r}_0|/h)}{\gamma^2\cosh(m)}\mathrm{d}m\left[1 - \cos\left(\gamma\sqrt{g/h}(t - \tau)\right)\right]. \tag{5.7}$$

Assuming a piston motion, $W_n(x, y, t) = \eta_b(x, y)\delta(t)$, the final expression for the water displacement is (Kajiura, 1963)

$$\eta(\mathbf{r}, t) = \frac{1}{2\pi h^2}\int\int \eta_b(\mathbf{r}_0)\mathrm{d}\mathbf{r}_0 \int_0^{+\infty} \mathrm{d}m\frac{mJ_0(m|\mathbf{r} - \mathbf{r}_0|/h)}{\cosh(m)}\cos\left(\gamma\sqrt{g/h}t\right). \tag{5.8}$$

Hence, at $t = 0$ we find the elevation of the water level caused by the piston motion of the basin bottom. The latter is used as initial value when solving the shallow-water wave equation (4.3)

$$\eta_0(x,y) = \frac{1}{2\pi h^2}\int\int \eta_b(x_0,y_0)\mathrm{d}x_0\mathrm{d}y_0 \int_0^{+\infty} \mathrm{d}m \frac{mJ_0(m|\mathbf{r}-\mathbf{r}_0|/h)}{\cosh(m)}. \tag{5.9}$$

We can see that the initial water displacement, generally speaking, does not repeat the bottom shift. Kajiura (1963) has performed specific calculations using (5.9). Particularly, for a homogeneous source of a circular shape the water displacement above the source center answers the bottom elevation at $R_e > (2-4)h$, i.e., in the framework of the usual assumptions of the shallow-water theory. The water displacement at the ends of the source is smoother than the bottom elevation and does not contain jumps as in the shallow-water approximation. Meanwhile, this effect is not essential for applications, and the tsunami source of the seismic origin can be determined in the shallow-water theory.

However, the finite-depth approximation changes radically the wave field far from the source if even if it is well described well in the theory by the shallow-water theory. Considering the 1D wave field out of the source area the Fourier transformation can be applied

$$\eta(x,t) = \int \eta(\omega)\exp\left[\mathrm{i}(\omega t - kx)\right]\mathrm{d}\omega, \tag{5.10}$$

where $\eta(\omega)$ is the frequency spectrum of the radiated wave (it can be found within the shallow-water theory), and the wavenumber, k and wave frequency, ω satisfy to the dispersion relation

$$\omega(k) = \sqrt{gk\tanh(kh)}. \tag{5.11}$$

In the shallow-water approximation, $\omega = ck$, where as early $c = (gh)^{1/2}$, and (5.10) gives the trivial answer, $\eta(x,t) = \eta(t - x/c)$, and the wave does not change its shape in the process of the wave propagation, as it is expected from (4.5). In the finite-depth approximation, water waves have dispersion, and the spectral components propagate with the different velocities resulting in a wave shape deformation. Considering almost long waves ($kh << 1$), the relation (5.11) can be simplified

$$k \approx \frac{\omega}{c}\left(1 + \frac{\omega^2 h^2}{6c^2}\right). \tag{5.12}$$

Asymptotic expression of the integral (5.10) with (5.12) for large distances from the source is expressed through the Airy function

$$\eta(x,t) = cH_0T_0\left(\frac{2}{h^2x}\right)^{1/3} Ai\left[\left(\frac{2}{h^2x}\right)^{1/3}(x-ct)\right], \tag{5.13}$$

which is plotted in figure 10 in normalized variables. Here H_0 and T_0 are the amplitude and duration of the wave radiated from the source. In fact, the value, cH_0T_0 can be replaced by V, the volume of the initial water displacement, and the solution (5.13) is valid for $V \neq 0$. So, the time record of the tsunami wave far from the source begins with the

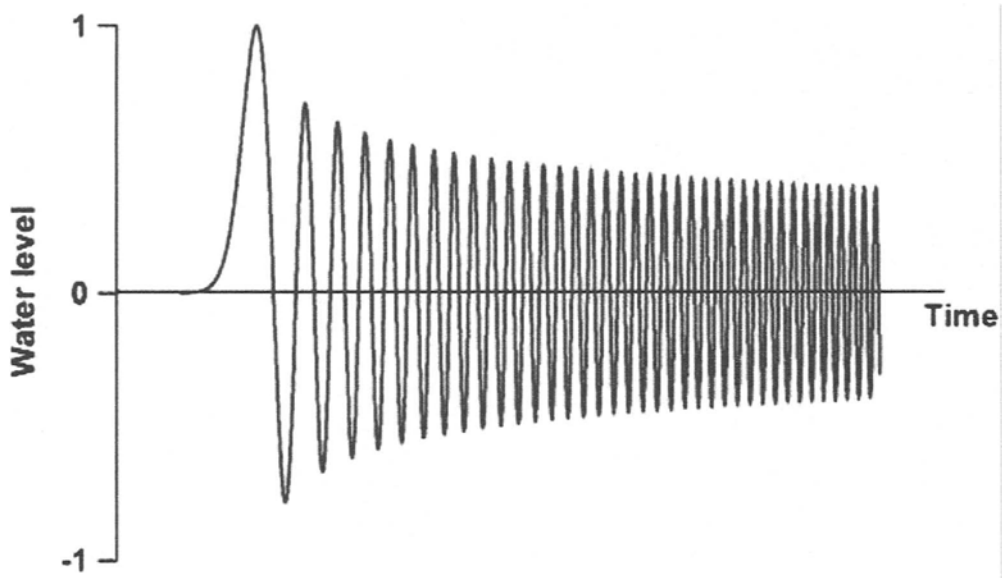

Figure 10. Time series of the dispersive wave (5.13) far from the source.

long wave accompanied by a train of smaller waves with decaying period. This is simply explained by the effect of dispersion, where the longer waves have larger propagation speed than the shorter. It is important to mention that the height of the leading wave is attenuated with distance as $x^{-1/3}$, and its duration grows as $x^{1/3}$. In the 2D case, far from the source, due to cylindrical divergence, the leading wave height is proportional to $r^{-5/6}$, and its duration - to $r^{1/3}$. If the earthquake generates the sign-variable disturbance with zeroth volume, V, the leading wave height is attenuated as $x^{-2/3}$ in the 1D case, and $r^{-7/6}$ in the 2D case. But in both cases the leading wave is not the wave of maximal amplitude. The asymptotic for the height of maximal amplitude is $x^{-1/2}$ (1D) and r^{-1} (2D), and for duration, $x^{1/2}$ or $r^{1/2}$; these formulas can be obtained by using the method of stationary phase.

We discussed above impulse (instantaneous) bottom displacements during the earthquake. Very often during the earthquake, the short and steep waves are exited in the epicentral zone. Seaquakes are followed by strong hydro-acoustic and cavitation effects, and they are dangerous for navigation in the open sea, unlike tsunami waves that are dangerous in coastal zones only. Amplitudes of the seismic oscillations are practically confined within the range 10^{-6} through 10^{-3} m, frequencies of such oscillations are 0.1 to 100 Hz, oscillation velocities, 10^{-3} through 0.1 m/s, acceleration, 0.1 through 10 m/s^2 (Aki and Richardson, 1980). Witnesses have reported that there appears on the sea surface a grid of waves with lengths 10-20 m and frequency 1 Hz during 10-60 s. The simplest model of a seaquake can be considered again with the use of (4.1) in the shallow-water approximation, or (5.6) taking into account the effects of the finite depth, if we

assume that the bottom elevation is a homogeneous rise in the band $|x| < L/2$ oscillating in time with frequency, ω . In particular, the wave field directly over the epicenter of the underwater earthquake in the shallow-water approximation is easily found from the Duhamel integral (4.15)

$$\eta(t, x = 0) = -\frac{2H_e}{\pi} \sin[\omega(t - L/4c)]. \tag{5.14}$$

It follows from (5.14) that at frequencies $\omega L/4c = \pi/2 + \pi n (n = 0, 1, ...)$ the amplitude of the water level oscillations practically coincides with the amplitude of bottom shifts. This resonance condition can be written in a more traditional form

$$L = cT_n(2n + 1), \tag{5.15}$$

and is fulfilled well for typical conditions of seaquakes. The finite-depth approximation leads to the decrease of the seaquake amplitudes.

Earlier we took into account the bottom motion only as "forcing" in the wave equation. However, the water depth varies also, and, therefore, we have equations with time-variable coefficients. The joint account of variability of the coefficients and external forcing is rather complicated. Therefore, we simplify the problem and assume the bottom shift to be homogeneous in space, $h = h(t)$. In this case we may in the governing Euler equations pass over to the system of coordinates connected with an oscillating bottom; and only equations (3.2) and (3.4) are changed by

$$\frac{\partial w}{\partial t} + \mathbf{u} \cdot \nabla_1 w + w\frac{\partial w}{\partial z} + \frac{1}{\rho}\frac{\partial p}{\partial z} = -g + \frac{\mathrm{d}^2 z_b}{\mathrm{d}t^2}, \tag{5.16}$$

$$w = 0 \qquad \text{at} \qquad z = -h, \tag{5.17}$$

where z_b is the ordinate of the bottom elevation. Thus, all the changes manifest themselves in re-normalization of the gravity acceleration. In the linear approximation for spatial Fourier harmonics the following ordinary differential equation can be derived (Rabinovich et al., 2000)

$$\frac{\mathrm{d}^2 Q}{\mathrm{d}t^2} + \left[g - \frac{\mathrm{d}^2 z_b}{\mathrm{d}t^2}\right] k \tanh(kh) Q = 0, \tag{5.18}$$

where $Q = \partial\eta(k, t)/\partial t$. In the specific case of the periodic bottom motions $z_b(t) = H_e \cos(\omega t)$, equation (5.18) reduces to the Mathieu equation and its general solution is expressed by the Mathieu functions. Under certain conditions between coefficients the solution grows exponentially, and parametric resonance occurs. This is possible under the following conditions

$$\sqrt{g k_n \tanh(k_n h)} = n\omega/2, \qquad (n = 1, 2, ...) \tag{5.19}$$

and determines wavenumbers of unstable waves. The wave increment, γ at the basic frequency $(n = 1)$ is

$$\gamma = \frac{\omega^3 H_e}{2g}. \tag{5.20}$$